# Angular Correlation of Annihilation Radiation in Various Substances*

G. LANG† AND S. DEBENEDETTI
*Carnegie Institute of Technology, Pittsburgh, Pennsylvania*
(Received July 1, 1957)

The angular correlations of gamma-ray pairs arising from positron annihilation in various solids have been observed. With good resolution, measurements of these angular distributions have been made for a wide variety of metallic elements, several ionic salts, several insulators, and a semiconductor. Some of the results from metals are accountable in terms of the Fermi-gas model of conduction electrons and the assumption of thermalized positrons.

Many metals exhibit angular distributions which differ singificantly from the Fermi-gas type, while retaining some of its features. For the noble and transition metals, however, the simple treatment is completely inadequate. Some possible theoretical interpretations of these distributions will be indicated. Measurements made on a group of alkali halides indicate the dominance of the halogen in determining the angular distribution, the width of which increases regularly with the chemical activity. The possibility of using positrons to study Pd–H alloys has been investigated. A measurement of positron mobility in diamond yielded a null result, within the accuracy of the experiment.

## INTRODUCTION

THE conduction electrons of a metal normally possess a kinetic energy of several ev. One would expect then that if a positron annihilates with an electron in a metal, the center of mass of the pair would not in general be at rest at the time of annihilation. Through the conservation principle, the momentum of the pair manifests itself in two ways: a slight departure from collinearity of the gammas would be caused by the component of momentum ($p_\perp$) perpendicular to the direction of emission, and unequal distribution of the energy between the gamma rays (Doppler shift) would result from the momentum component ($p_{\parallel}$) in the direction of emission. Quantitatively these effects are:

$$\sin\theta \approx p_\perp/mc, \tag{1}$$

$$\Delta E \approx \tfrac{1}{2} p_{\parallel} c, \tag{2}$$

where $mc^2+\Delta E$ and $mc^2-\Delta E$ are the energies of the gamma rays and $(\pi-\theta)$ is the angle between them. While $E$ is rather difficult to measure accurately, the relative ease of measuring $\theta$ facilitates its use in investigating electronic motion in solids.

The first measurements of this type were made in 1949 by DeBenedetti, Cowan, Konneker, and Primakoff,[1] who observed the angular distribution of gamma pairs from Au. Since that time a number of investigators have applied the method to a variety of solids.[2–9]

The question of thermalization of the positrons is of course of considerable importance in the interpretation of gamma-pair angular distributions. The lifetime of positrons in solids has been measured, and is at least $1.5\times10^{-10}$ in all of the measured materials.[10] Theoretical treatments of thermalization time have undergone progressive refinement, the treatment of Lee-Whiting[11] yielding an estimated thermalization time of $3\times10^{-12}$ in metals, a value considerably shorter than the annihilation lifetime. Probably the most significant supporting experimental result is the fact that the gamma-pair angular distributions from light metals are explainable in terms of thermalized positrons.

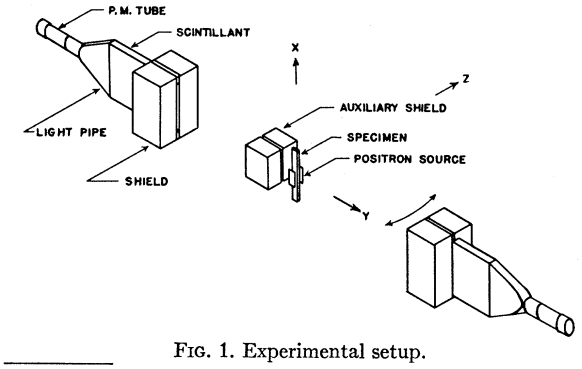


FIG. 1. Experimental setup.

## EXPERIMENTAL APPARATUS

The physical arrangement of the experimental apparatus is shown in Fig. 1. Each counter aperture is located two meters from the specimen, and is 2 mm wide by 12.7 cm high. The specimens are usually 1 mm thick; some are folded so as to have an apparent

* This work was supported by a National Science Foundation Grant.

† National Science Foundation Fellow during the period of this investigation.

[1] DeBenedetti, Cowan, Konneker, and Primakoff, Phys. Rev. **77**, 205 (1950).
[2] P. E. Argyle and J. B. Warren, Can. J. Phys. **29**, 32 (1951).
[3] J. B. Warren and G. M. Griffiths, Can. J. Phys. **29**, 325 (1951).
[4] H. Mayer-Leibnitz, Z. Naturforsch. **6(a)**, 663 (1951).
[5] Ambrosino, Houbaut, and Maignan, Compt. rend. **237**, 708 (1953).
[6] R. E. Green and A. T. Stewart, Phys. Rev. **98**, 486 (1955).
[7] Page, Heinberg, Wallace, and Trout, Phys. Rev. **98**, 206 (1955).
[8] A. T. Stewart, Phys. Rev. **99**, 594 (1955).
[9] Lang, DeBenedetti, and Smoluchowski, Phys. Rev. **99**, 596 (1955).
[10] R. E. Bell and R. L. Graham, Phys. Rev. **90**, 644 (1953).
[11] G. E. Lee-Whiting, Phys. Rev. **97**, 1557 (1955).

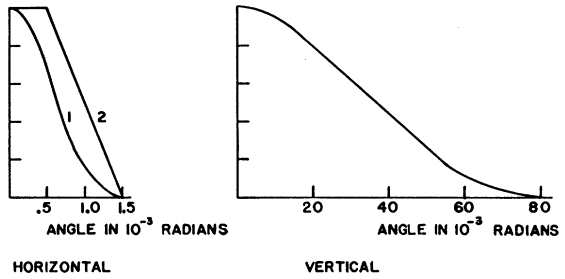


FIG. 2. Resolution functions of the apparatus. The two extreme possibilities are shown for the horizontal resolution.

thickness of 1 mm. Since the positron source is not incorporated in the sample, the latter is easily changed. The auxiliary shield prevents the fixed counter from seeing the radioactive material; because the counters are operated in coincidence, only one such shield is needed. In order to minimize the stability requirements imposed by low counting rates, an automatic device collects data by passing through a schedule of counter positions rapidly and frequently. The electronic apparatus is of a standard type and does not merit discussion here.

It will be noted that the apparatus does not measure $\theta$, the angle between gamma pairs, but rather $\alpha$, the projection of this angle on the $yz$ plane. Since the vertical resolution is much broader than any observed angular distribution, the instrument is sensitive essentially only to the $z$ component of the momentum of the annihilating pair. The horizontal resolution varies slightly with the form and density of the sample. Both resolutions are shown in Fig. 2.

## FERMI GAS MODEL

The $z$ component of the pair momentum measured in units of $mc$ is equal to the angle $\alpha$ in radians. In angular distributions from polycrystalline materials, the measured result is an average over all orientations of the crystal structure with respect to the apparatus. Under these conditions we can relate $N_z(p_z)$, the distribution in $z$ momentum, to $N(p)$, the distribution in magnitude of momentum, by the following simple relation:

$$N_z(p_z)=\tfrac{1}{2}\int_{p_z}^{\infty}\frac{N(p)}{p}dp. \tag{3}$$

The simplest model of a metal is the one in which the valence electrons are assumed to behave as a Fermi gas. In the approximation of zero temperature this model yields

$$\begin{aligned} N(p)&=p^2 \quad \text{for} \quad p^2<p_m^2 \\ &=0 \quad \text{for} \quad p^2>p_m^2, \end{aligned} \tag{4}$$

where $p_m=h(3n_0/8\pi)^{\frac{1}{3}}$, $n_0$ being the electron density. If we make the simplifying assumptions that the positron has negligible momentum and that the probability of annihilation is independent of electron momentum, the corresponding distribution in $p_z$ becomes

$$\begin{aligned} N_z(p_z)&=(p_m^2-p_z^2) \quad \text{for} \quad p_z^2<p_m^2 \\ &=0 \quad \text{for} \quad p_z^2>p_m^2. \end{aligned} \tag{5}$$

The relation between $N_z$ and $N$ in this case may also be visualized geometrically. The occupied electronic states are uniformly distributed within a sphere of radius $p_m$ in momentum space. The measuring apparatus cuts from this sphere slices which are of standard thickness and which are bounded by planes perpendicular to the $p_z$ axis. The volume of a slice, and hence the number of its included electronic states, depends upon its distance from the origin and is proportional to $(p_m^2-p_z^2)$. The distribution has the form of an inverted parabola.

On the basis of the angular distribution which each exhibits, the metals conveniently may be classified into three groups. Group $A$, comprising Li, Na, Be, Mg, Al, Ge, Sn, and Bi, have distributions composed of central inverted parabolas with small tails at large angles. Group $B$, comprising Ca, Ba, Zn, Cd, and Pb, again have the central parabolas, but have larger tails. The distinction between Groups $A$ and $B$ is somewhat arbitrary. The group $C$ metals, Cu, Ag, Au, Fe, Co, Ni, Rh, Pd, Pt, and W, exhibit bell-shaped angular distributions.

The angular distributions for most of the metals of group $A$ have appeared in a previous publication.[9] Those for the two additional members, Ge and Bi, are shown in Figs. 3 and 4. In fitting the theoretical parabolas to these data, the following procedure is used. Each distribution is considered to consist of a central parabolic part and a small tail at large angles. A parabola and a tail are roughly drawn through the experimental points. At the intersection of these curves, a horizontal line is drawn, forming a pedestal upon which the theoretical parabola is placed. The curves finally shown are computed parabolas adjusted

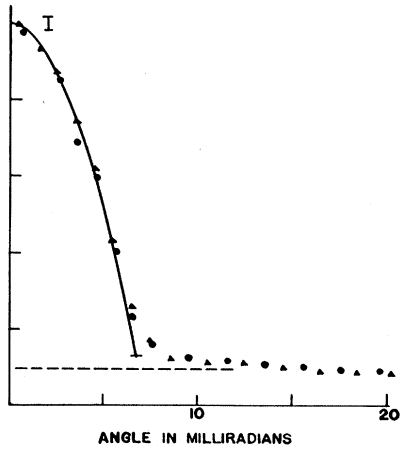


FIG. 3. Angular distribution from Ge; dashed line indicates background of random coincidences.

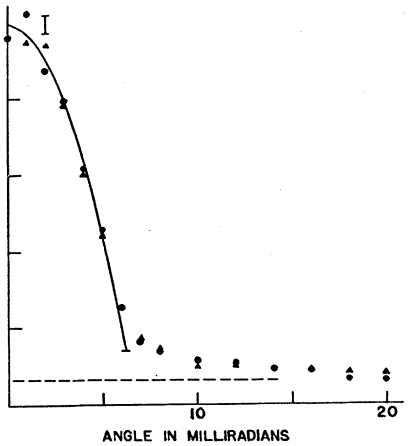


FIG. 4. Angular distribution from Bi; dashed line indicates background of random coincidences.

in height to fit the data and in width to fit the Fermi-gas model, using a number of free electrons per atom equal to the number of the group in which the metal appears in the periodic table. The reason for this construction lies in the form of expression (3). It is apparent that $N_z$ must be a monotonically nonincreasing function of $p_z$. Thus, if it were possible to observe separately the "tail-producing" type of annihilations, their $N_z$ curve would never have a minimum. It is of course possible that it would be concave downward rather than flat for $p_z<p_m$. The background caused by random coincidences is shown as a horizontal dashed line in Figs. 3 and 4. It is interesting to note that Ge, a semiconductor, can be so well represented by the Fermi-gas model. Distributions from samples with impurity concentrations ranging between $10^{13}$ and $10^{18}$ taken at temperatures between $-78°$ and $+100°$C displayed no noticeable differences. This is not unreasonable, for the positrons apparently sample the entire valence band and are thus relatively insensitive to those few electrons at the band edge which have such profound effects upon electrical properties.

The parabolic parts of the distributions from group-$A$ metals may be made linear by plotting the counting rate against the square of the angle. By drawing a straight line through the linear region of each plot and finding its intersection with the pedestal found according to the method of the previous paragraph, we can determine the measured value of $p_m$. The results of such operations are summarized in Table I. In the column labeled "Measured valence" are shown the number of free electrons per atom necessary to give the measured $p_m$ in the Fermi-gas model.

## REFINEMENTS OF THE MODEL

We now consider the possibility of refining our model and hence its predicted angular distribution. Deviations from the parabolic distribution shape possibly may be caused by one or more of the following effects: 1. The positrons are not thermalized. 2. The probability of annihilation is not independent of the relative velocity of positron and electron. 3. The Fermi surface is not spherical. 4. The positrons annihilate with core electrons as well as with valence electrons. 5. The positrons, although thermalized, have significant zero-point motion because they are confined by the periodic potential of the lattice (excluded-volume effect).

Considering the success of the Fermi-gas model in the case of group-$A$ metals, we regard (1) and (2) as probably unimportant. Effect (3) could hardly account for the high momentum values in the tails of group $C$. The similarity of the Cu, Ag, and Au distributions would seem difficult to reconcile with (4) since their core radii vary considerably ($1.15a_0$, $1.74a_0$, and $2.04a_0$, respectively). We certainly do not wish to exclude the possibility of a core-electron annihilation on such a meager basis, but we will concentrate our attention upon the application of (5). It will be found that this effect alone is not sufficient to account for all the experimental observations, although it does offer a possible explanation of the similarity of the monovalent noble-metal distributions.

In the treatment of the excluded-volume effect, we adopt and extend the method developed by Primakoff.[1] In this model the core repulsions are approximated by assuming that there exists about each metal ion a spherical region of volume $v_e$ from which the positrons are excluded. In the interstitial regions positrons and electrons are represented by plane waves. The amplitude for annihilation of a positron of wave number $\mathbf{k}_+$ with an electron of wave number $\mathbf{k}_-$ and the creation of a gamma pair with total momentum $\mathbf{p}$ is given [see Eq. 11, reference 1] by the following expression:

$$\Phi_{k+,\,k-}(\mathbf{p})=(2\pi)^3\sum_{\mathbf{g}}\left[\delta_{g,0}-\frac{v_e}{v_i}\left\{3\frac{\sin 2\pi g r_e-2\pi g r_e\cos 2\pi g r_e}{(2\pi g r_e)^3}\right\}\right]\times\delta(\mathbf{k}_++\mathbf{k}_-+2\pi\mathbf{g}-\mathbf{p}). \quad (6)$$

Here $r_e$ is the radius of $v_e$, $v$ is the unit cell volume, and the $\mathbf{g}$'s are reciprocal lattice vectors.

TABLE I. Comparison with the Fermi gas model.

| Metal | Group | Computed $p_m$ | Measured $p_m$ | Measured valence |
|---|---|---|---|---|
| Li | I | 4.27 | 4.3 | 1.0 |
| Na | I | 3.50 | 3.6 | 1.1 |
| Be | II | 7.48 | 7.4 | 1.9 |
| Mg | II | 5.27 | 5.3 | 2.1 |
| Al | III | 6.74 | 6.7 | 3.0 |
| Ge | IV | 6.69 | 6.8 | 4.2 |
| Sn | IV | 6.29 | 6.4 | 4.2 |
| Bi | V | 6.21 | 6.1 | 4.7 |

If now we set $\mathbf{k}_+$ equal to zero and assign to the electrons a wave number distribution corresponding to that of a Fermi gas, it is possible to prescribe a recipe for finding the probability of observing a gamma pair of momentum **p**. Imagine each point of the reciprocal lattice (in $k$ space) surrounded by a sphere of radius $k_m$, where $k_m$ is the maximum wave number of the Fermi gas. For convenience we will refer to these as $k$ spheres. To each $k$ sphere assign a number $\Phi$ which depends on the distance from the origin to its center. Now draw the vector **p** with its tail at 0. If the head of this vector lies within one of the $k$ spheres, the probability of observing a gamma-ray pair with momentum **p** is proportional to the square of the value of $\Phi$ associated with that sphere. If the head of the vector lies within more than one sphere, the respective values of $\Phi$ must be added and the sum must be squared. A zero probability is indicated if the head of **p** does not lie within any $k$ sphere.

### APPLICATION OF THE EXCLUDED VOLUME EFFECT TO Cu, Ag, AND Au

We first consider the application of the preceding calculation to the case of Au. Here the $k$ spheres do not overlap. The reciprocal lattice is body-centered cubic (b.c.c.). $N(p)$ may be found by using the recipe which has already been described and summing over all orientations of the vector with magnitude $p$. This has been done for several values of the parameter $v_e/v$. A numerical treatment was used up to $p_z=19\times10^{-3}$ $mc$; beyond this an approximate analytical method was used. A numerical integration of (3) yields the $N_z(p_z)$ curves which, together with the experimental points, have been plotted in Fig. 5. Note that each theoretical curve consists of a central parabola (from the $g=0$ term of the probability-amplitude expression) which is placed on a flat-topped pedestal. The notch would be at least partially smoothed out for a non-spherical Fermi surface. There are some small irregularities in the curves of the tails. These have not been drawn in the figure because they were not well resolved by the approximate numerical method used.

TABLE II. Analysis of parabolic and gaussian parts of some distributions.

| Metal | $A_g/A_p$ | $v_e/v$ |
|---|---|---|
| Li | 0.21 | 0.15 |
| Na | 0.23 | 0.16 |
| Be | 0.062 | 0.05 |
| Mg | 0.12 | 0.10 |
| Al | 0.15 | 0.11 |
| Ge | 0.13 | 0.10 |
| Sn | 0.23 | 0.16 |
| Bi | 0.20 | 0.14 |
| Ca | 0.37 | 0.21 |
| Ba | 0.67 | 0.29 |
| Zn | 0.48 | 0.24 |
| Cd | 0.49 | 0.25 |
| Pb | 0.33 | 0.20 |

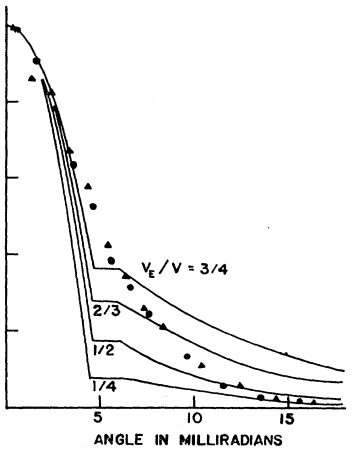


FIG. 5. Au: theoretical curves and experimental points.

From a comparison of the theoretical and experimental points several significant conclusions may be drawn. In order to account for the large values of the experimental counting rate in the region from 5 to 10 milliradians, one must assume an excluded volume of approximately $\frac{3}{4}v$. This is to be compared with the value of $0.31v$ which is obtained by setting $r_e=r_i$, where $r_i$ is the radius of peak probability density for the outer electronic shell of the free ion.[12] The similarity of the measured distributions from Cu, Ag, and Au indicates that they would all require about the same value of $v_e/v$, although the values of $v_i/v$ are 0.08, 0.19, and 0.31, respectively.

Suppose that in the three metals which we are considering, the positron never penetrates the ions sufficiently to see their detailed structure. The external ionic field which it would see would be a Coulomb field characterized merely by the ionic charge. The similarity of the distributions would then seem reasonable, for the ionic charge is the same in each case. In addition, since the positron would see a Coulomb field, a gradual cutoff of its wave function would be more appropriate than the sharp cutoff which we postulated in the calculation. The gradually attenuated wave function would have reduced high-momentum components, and the $N_z$ calculated from it would have a lower value at large $p_z$, making it a better representation of the experimental results. Here we have an agrgument which is at least internally consistent and which accounts at the same time for the general shape of the monovalent noble-metal distributions and the similarity of them. Evidence which appears to contradict it, or at least its application to metals in general, is presented below.

We now attempt to apply the excluded-volume model to the metals of groups $A$ and $B$. For small values of $v_e/v$ it is possible to calculate $N_z$ by an approximate analytical method. This yields an $N_z$ composed of a broad Gaussian curve surmounted by a central parabola.

[12] J. C. Slater, Phys. Rev. **36**, 57 (1930).

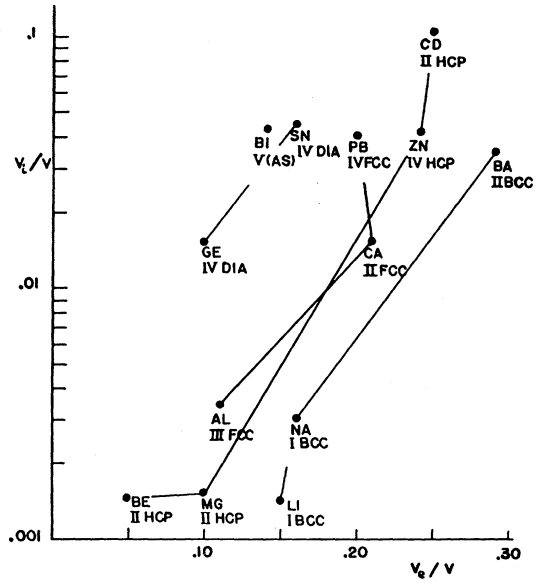


FIG. 6. Comparison of ionic volumes and required excluded volumes.

The ratio of the areas of the Gaussian and parabolic parts is given by the following approximate expression:

$$\frac{A_g}{A_p}=\frac{(5\sqrt{5})\pi v_e/v}{6\pi(1-2v_e/v)}\approx\frac{v_e/v}{1-2v_e/v}. \tag{7}$$

The measured distributions of groups $A$ and $B$ have been resolved roughly into parabolic and Gaussian parts; the area ratios have been found, and the corresponding values of $v_e/v$ have been determined. The pertinent information is shown in Table II. These values of the volume ratio, which should be regarded as about 20% accurate, have been plotted (Fig. 6) against $v_i/v$, which is found from the outer ionic shell radius, in the hope of observing some regularities. The valence and crystalline type have also been indicated on the plot. The first noteworthy feature is that $v_e/v$ does not appear to increase with the ionic charge in any regular manner, a feature which we would expect if the positrons saw only the external (Coulombic) ion fields. There does seem to be some correlation between the two volume ratios, although they differ by orders of magnitude in some cases. There is a regularity involving the crystalline types. If all the points referring to material of the same crystalline type are joined by lines in the order of increasing $v_i/v$, these lines slope generally to the right and are arranged as As, diamond, f.c.c., h.c.p., and b.c.c., in order of increasing $v_e/v$. It appears that there is correlation between the volume ratios within a given crystalline type.

It is apparent that our attempts to account for the angular distributions of annihilation radiation from metals leave much to be desired. We have considered in detail only one possible refinement of the Fermi-gas model, and the conclusions drawn from it do not agree with all the experimental results. We hope that we have achieved the minimum goals of provoking thought

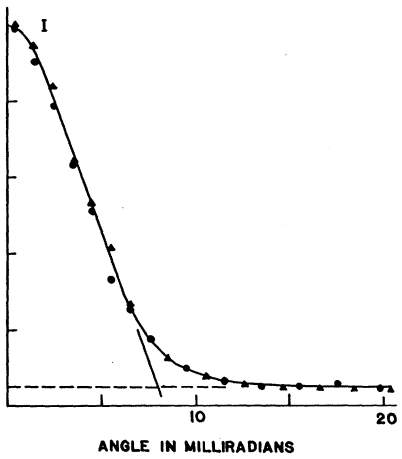


FIG. 8. Angular distribution from NaCl.

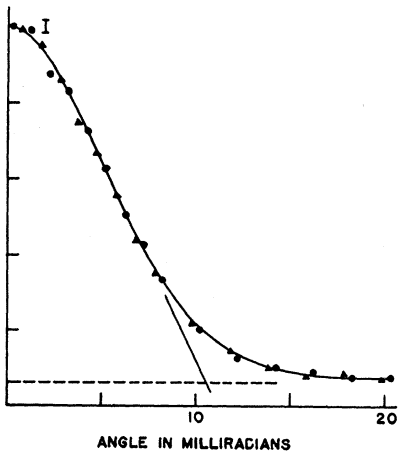


FIG. 7. Angular distribution from LiF.

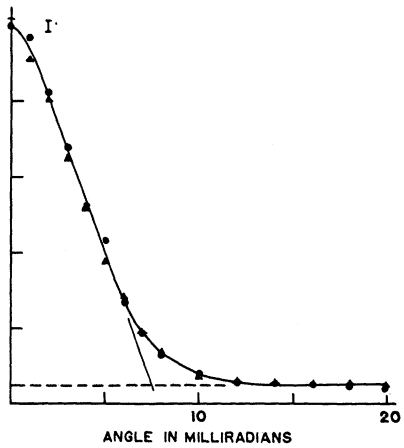


FIG. 9. Angular distribution from KCl.

TABLE III. Alkali halides—predictions of the localized treatment.

| Material | Predicted intercept | Measured intercept |
|---|---|---|
| LiF | 10.9 | 10.6 |
| NaCl | 8.00 | 8.0 |
| KCl | 8.00 | 7.5 |
| KI | 6.58 | 6.7 |

on this subject and of indicating some possible directions for further work.

## ALKALI HALIDES

A positron in an ionic crystal should be attracted to the negative ions. For this reason, it has been predicted[1] that the angular distribution of annihilation radiation from alkali halides should be determined largely by the halogen atoms, and should vary in width with their chemical activity. In order to test this prediction, measurements were made on LiF, NaCl, KCl, and KI. The LiF sample was made of several large crystals, each with its cleavage planes perpendicular to the $z$ direction. The other three samples were polycrystalline aggregates with random orientation. The measured distributions (Figs. 7–10) are more or less triangular in shape. If the straight sides of these curves are extended downward to intercept the background, the abscissas of these intercepts may be used to characterize the distribution widths. The prediction mentioned above seems to be verified. Ferrell[13] has, in fact, accounted for the intercept values by considering the binding of a positron to a free halogen ion. His theory predicts an intercept at $p_z=14.48/a$, where $p_z$ is in units of $10^{-3}$ $mc$ and $a$ is the Goldschmidt radius in angstroms. In Table III Ferrell's predictions are compared with the measured values. It appears that the distributions are almost completely determined by the character of the halogen constitutent, but before regarding this as a closed case, one should consider the following argument.

If we could compress a system in real space, its representation in momentum space would expand in the same proportion. Consider what would happen to the NaCl distribution if we were to squeeze or stretch NaCl and cause it to have the same lattice constant as each of the other measured materials in turn. As Table IV shows, the intercepts of the other three materials are fairly well reproduced. Thus the possibility of interpreting the distributions in terms of characteristics of the whole crystal is not entirely ruled out. A comparison of LiF and CsF, in which the interatomic spacings are in the ratio 2:3, should be illuminating.

TABLE IV. NaCl distribution width adjusted for lattice constant.

| Material | Adjusted NaCl intercept | Measured intercept |
|---|---|---|
| LiF | 11.2 | 10.6 |
| NaCl | 8.0 | 8.0 |
| KCl | 7.2 | 7.5 |
| KI | 6.3 | 6.7 |

[13] R. A. Ferrell, University of Maryland Physics Department. Technical Report No. 43 (unpublished).

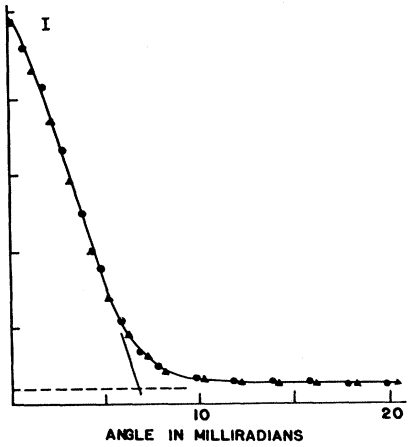


FIG. 10. Angular distribution from KI.

## POSITRON MOBILITY IN DIAMONDS

The angular distribution of annihilation gamma rays from diamond is shown in Fig. 11. The shape of the distribution appears to lie between the parabolic shape of metals and semiconductors and the triangular shape which characterizes most insulators.

The mobility of electrons in diamonds has been found[14] to be as high as several thousand cm²/volt-second in some samples. It was thought that positrons might also have high mobility, and an experiment was devised to investigate this possibility by means of observations on the angular distribution of annihilation gamma-ray pairs. If one applies an electric field $E$ to a material which contains mobile positrons, these particles will acquire a drift velocity $v_d$ in the direction

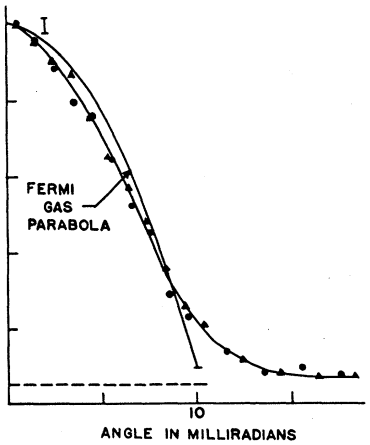


FIG. 11. Angular distribution from diamond.

[14] E. A. Pearlstein and R. B. Sutton, Phys. Rev. **79**, 907 (1950).

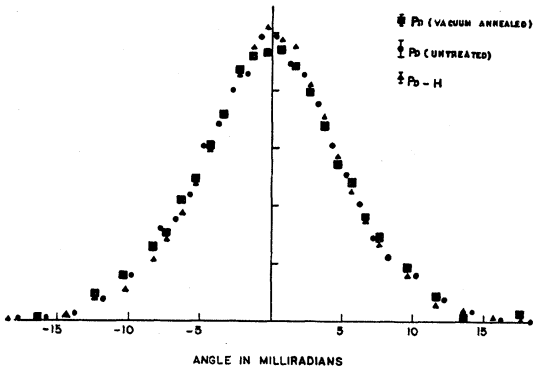


FIG. 12. Angular distribution from Pd and Pd—H.

of the field. The drift should cause a shift $\delta\alpha$ of the entire gamma-pair angular distribution, for (in insulators) the field will not alter the momentum distribution of the electrons of the material. The magnitude of $\delta\alpha$ will be equal to $v_d/c$, where $c$ is the velocity of light. The mobility is then simply given by $c(\delta\alpha)/E$.

For the experiment, a dozen small flat diamonds were mounted in such a way that they could be placed in the angular-correlation apparatus and bombarded from one side by one of the positron sources. A very thin layer of Aquadag was painted on the faces through which the positrons entered, and a 60-cycle potential of 1000 volts rms was applied between this and the metallic diamond supports. The counter slits were opened to 4 mm and the data recorder was set to make counts at $-5$, 0, and $+5$ milliradians, stopping at each point for eight minutes and completing a cycle in approximately 50 minutes. The coincidences signals were passed through a gating circuit which fed two scalers in such a way that scaler $A$ operated while the field in the diamonds was to the right, and scaler $B$ operated while the field was to the left. The results of a 4-day run are shown in Table V. The slope of the distribution curve at zero is of course zero, so that we should expect total counts $0-A$ and $0-B$ to be equal. The counts are not equal because the source was not at the same potential as the adjacent diamond faces: the slower positrons were repelled away from the diamonds during the $A$ half of the cycle. The slope of the angular distribution at 5 milliradians is such that the counting rate changes about 15% per milliradian (see Fig. 11). This means that distribution $A$ was shifted to the right by $0.073\pm0.100$ milliradian with respect to distribution $B$. The average thickness of the diamonds was 1 mm, so that the average field in each direction was approximately $(2\sqrt{2}/\pi)\times(1000/0.1)=9000$ volts/cm. The resultant measured positron mobility was thus $[(0.073\pm0.100)\times10^{-3}c]/(2\times9000)=120\pm160$ cm$^2$/volt sec. This result, though it is in the correct direction, is well within statistics and therefore there is practically no evidence of positron motion.

TABLE V. Positron mobility experiment.

| Angle | Scaler | Total counts | $(B/A)$ | $(B/A)/(B/A)_0$ |
|---|---|---|---|---|
| $-5$ | $A$ | 7823 | $1.063\pm0.016$ | $1.006\pm0.021$ |
| $-5$ | $B$ | 8319 | | |
| 0 | $A$ | 11368 | $1.057\pm0.013$ | |
| 0 | $B$ | 12010 | | |
| 5 | $A$ | 8054 | $1.041\pm0.016$ | $0.984\pm0.021$ |
| 5 | $B$ | 8390 | | |

Faced with the null result of the mobility experiment, we consider the possibility that the positrons do not exist long enough to acquire their terminal drift velocity. The relaxation time, which characterizes the rapidity of a particle's response to an impressed field, is proportional to the mobility. For a positron or an electron with a mobility of 1000 cm$^2$/volt sec, the relaxation time is less than $10^{-12}$ second. Comparing this with the mean life of roughly $10^{-10}$ second, we see that there is ample time for the acceleration of the positron before its annihilation.

The electron mobilities in the samples which were used had not been determined—a new experiment utilizing carefully selected diamond samples is now being planned. It is of course not unreasonable that positron and electron mobilities in the same sample might differ significantly. The most obvious possibility is that positrons might fall into bound states (other than positronium) and thus be completely immobile. Although no measurements have been made to detect positronium in diamond by means of its effect on the three-quantum annihilation rate, the lack of a long-lived component in the positron lifetime[10] seems to exclude its existence. It is possible that positrons are more effectively scattered than electrons because of fundamental differences in their interactions. It is well known that the scattering cross section of an attractive potential can differ materially from that of a repulsive potential of the same shape. In addition, positron-electron interactions differ from electron-electron interactions in that exchange effects are not present in the former.

## OCCLUSION OF HYDROGEN IN PALLADIUM

An attempt was made to observe the effect of occluded H upon the gamma-pair angular distribution from Pd. Hydrogen was introduced into a Pd sample electrolytically, the resistivity change of the sample indicating the presence of 0.7 H atom for each atom of Pd. The angular distribution from this sample was then recorded and is shown as the circular points of Fig. 12. After annealing in vacuum at 400°C for 2 hours, the resistivity returned to its normal value, and the distribution shown by the square points of Fig. 12 was measured. The triangular points of the same figure refer to an untreated Pd specimen; all

distributions are normalized to the same total number of counts. Since no gross effects were observed, the investigation was discontinued in favor of other work. These preliminary results have been included here because they may be of use to other investigators. In particular, they indicate that if the angular correlation method is to be of use in the study of Pd—H alloys, rather precise measurements with good statistics will be required.

ACKNOWLEDGMENTS

The authors wish to thank Professor S. Friedberg, Professor W. Kohn, Professor P. Marcus, and Professor R. Smoluchowski for many valuable suggestions and discussions.

PHYSICAL REVIEW VOLUME 108, NUMBER 4 NOVEMBER 15, 1957

# Electrical Resistivity of the Ni—Pd Alloy System between 300°K and 730°K

A. I. SCHINDLER, R. J. SMITH, AND E. I. SALKOVITZ
*Metallurgy Division, United States Naval Research Laboratory, Washington, D. C.*
(Received July 22, 1957)

Electrical resistivity measurements have been made on alloys of Ni and Pd from room temperature to 730°K. The maximum in the resistivity was found to shift from 70 atomic percent Pd 30 atomic percent Ni at room temperature, to the 50–50 composition at temperatures where all the specimens are paramagnetic. At these elevated temperatures it was found that Matthiessen's rule is obeyed over the entire range of compositions. The general behavior may be interpreted in terms of the dependence of *s-d* scattering upon temperature and composition.

## INTRODUCTION

ELECTRICAL resistivity measurements between 300°K and 730°K for the Ni—Pd alloy system will be discussed in this paper. Preliminary measurements between 4.2°K and 300°K have already been published for this system.[1] The results showed that at the low temperatures the resistivity is a maximum at 70 atomic percent Pd. This was explained by splitting up the resistivity into two parts: one, $\rho_{s\text{-}s}$, resulting from *s-s* scattering, and one, $\rho_{s\text{-}d}$, resulting from *s-d* scattering, and then considering how these parts varied with composition. Ni is ferromagnetic up to 629°K and Pd is paramagnetic at all temperatures. Both elements contain 0.6 hole in their respective *d* bands (3-*d* for Ni and 4-*d* for Pd) and 0.6 conduction electrons in the *s* bands (4-*s* for Ni and 5-*s* for Pd). It is reasonable to assume that the number of *s* electrons remains constant with composition at 0.6[2] and consequently $\rho_{s\text{-}s}$ will vary in a Nordheim manner,[3] i.e., as $x(1-x)$, where $x$ is the fraction of Pd atoms. While the number of holes in the *d* band is 0.6 for each composition, the effective number of Bohr magnetons, calculated from magnetization data, changes from a maximum for pure Ni to zero for 97 atomic percent Pd. This implies that the filling of the two half *d* bands changes gradually with composition from Ni to Pd. Half of the *d* band for Ni is completely filled and the other half contains 0.6 hole, thus allowing electrons of only one spin state to contribute to *s-d* scattering. In Pd both halves of the *d* band are equally populated with the same number of holes, so that electrons of both spins may be scattered from *s* to *d* states.

The total resistivity has been represented by Overhauser and Schindler[4] as

$$\rho=\frac{x(1-x)(S+Dq\uparrow^{p})(S+Dq\downarrow^{p})}{2S+Dq\uparrow^{p}+Dq\downarrow^{p}}, \qquad (1)$$

where $x$ is the Pd content, $q\uparrow$ and $q\downarrow$ are the number of holes in the spin-up and spin-down portions of the *d* band respectively, $S$ and $D$ are terms independent of composition referring to *s-s* and *s-d* transitions and $p$ is related to the band shape and is approximately unity. An examination of Eq. (1) reveals that since $q\uparrow$ and $q\downarrow$ are in general functions of composition, an asymmetrical variation of $\rho$ with composition is to be expected. However, when $q\uparrow$ is equal to $q\downarrow$ and is composition-independent, then $\rho$ varies as $x(1-x)$ and $\rho$ is consequently symmetrical about the 50–50 composition. This is equivalent to the earlier prediction of the authors[1] that the Nordheim relation should be applicable in the region where all of the alloys are paramagnetic, i.e., above the Curie temperature of nickel.

## EXPERIMENTAL PROCEDURE AND RESULTS

The resistivity measurements between 300°K and 730°K were carried out with the specimens in a vacuum. The temperature gradient did not exceed 0.25°C between the potential leads, which were approximately

[1] Schindler, Smith, and Salkovitz, J. Phys. Chem. Solids **1**, 39 (1956).
[2] E. P. Wohlfarth, Proc. Leeds Phil. Lit. Soc. Sci. Sect. **5**, 89 (1948).
[3] L. Nordheim, Ann. Physik **9**, 607 (1931).
[4] A. W. Overhauser and A. I. Schindler, J. Appl. Phys. **28**, 544 (1957).